The 6th International Conference on
Structural Health Monitoring of Intelligent Infrastructure
Hong Kong | 9-11 December 2013

PERFORMANCE MONITORING OF CEMENT GROUTED SOIL NAILS IN CUT SLOPES USING FIBER BRAGG GRATING SENSORS

C.Y. Hong [1], J.H. Yin [2], H.F. Pei [3], and P Lin[1]
[1] Department of Civil Engineering, Shantou University, Shantou, China. Email: joeyhcy@gmail.com
[2] Department of Civil and Environmental Engineering, The Hong Kong Polytechnic University, Hong Kong, China, Email: jian-hua.yin@polyu.edu.hk
[3] Department of Civil and Environmental Engineering, The Hong Kong University of Science and Technology, Hong Kong , China, Email: 08902616r@connect.polyu.hk

ABSTRACT

Soil nailing is commonly used as a permanent reinforcement technique for slopes, excavations and retaining walls. The long-term stability problems of a soil nailing system depends on the mechanical behavior of soil nails, particularly the axial tension force distributions along the axial directions of soil nails (or related friction resistance at the nail-soil interface). The measurement of axial force distributions of soil nails in slopes is therefore critical for researchers and engineers to carry out comprehensive analysis of slope stability problems. This paper describes a field research program for the measurement of the axial force distributions of cement grouted soil nails in permanent slopes. This research program lasted 4 to 6 months monitoring the mechanical behavior of a total of 42 soil nails in 7 permanent slopes. Strain information of all these soil nails was measured using fiber Bragg grating (FBG) strain sensors. Temperature compensation was also conducted for all these soil nails. Typical installation methods of strain and temperature sensors and the related protective measures of optical fiber cables and optical fiber sensors are introduced. Measured strain results were presented and analyzed to investigate how axial forces of soil nails formed and developed after grouting, and their relevance associated with the field construction works. The possible ground movement inside slope and its effect on the axial strain results of soil nails are also interpreted and discussed in the paper. All the measurement data are useful for a better understanding of the short-term and long-term behavior of cement grouted soil nails in a real field.

KEYWORDS

Soil nailing, axial tension force, strain information, FBG.

INTRODUCTION

Soil nailing is commonly used as a both permanent and temporary reinforcement technique for slopes, excavations and retaining walls. The long-term stability of a soil nailing system depends on the mechanical behaviour of soil nails inside geotechnical engineering structures. It is generally believed that the soil nail enhances the stability of soil mass principally by mobilizing the friction resistance at the nail-soil interface (or axial tension stress) (Jewell, 1991; Jewell, 1991; Plumelle et al., 1990). For a soil nailing system under service loading condition, the general consensus among researchers appears to be that, the soil nail is mainly subjected to effect of tension force. Even when failure condition occurs, the contribution of bending/shear effect is still limited compared with the axial tension force. Therefore, the measurement of the axial tension force distributions of soil nails in slopes is important to both researchers and engineers. The measurement of the mechanical behaviour of soil nails using different measurement technologies have been developed for many years and fiber Bragg grating (FBG) sensor is a popular one with a number of distinct advantages (Cheung and Lo, 2011; Hong et al., 2010). Other technologies such as, Low Coherence Interferometry (LCI), Brillouin Optical Time Domain Analysis (BOTDA) technique, and Brillouin Optical Time Domain Reflectometry (BOTDR) are also used as measurement methods for geotechnical engineering structures (Klar et al., 2006; Mohamad et al., 2011; Sun et al., 2010; Wu et al., 2008).

Laboratory test is a common method to evaluate the soil nail behaviour under different testing conditions by varying a number of factors, such as grouting pressures, overburden soil pressures, saturation conditions, etc (Su et al., 2007; Su et al., 2008; Yin and Zhou, 2009; Yin and Su, 2006). Since testing conditions of these soil nails in laboratory have been strictly controlled, a number of typical conclusions have been obtained, for example, correlations between pullout resistance (or axial force) of soil nails and several critical parameters, such as overburden soil pressure (soil depth), soil water content, grouting pressure, etc (Chu, L. M. and Yin, J. H., 2005; Chu, L.M. and Yin, J.H., 2005; Su et al., 2008; Yin and Zhou, 2009). For the complicated field tests, due to the complicated ground conditions and relevant testing uncertainties, the full-scale field test is seldom considered for a systematic study of the soil nail behaviour. Few typical studies show that the field pullout behaviour of cement grouted soil nails are complicated and uncertain (Zhang et al., 2009). Therefore, the field performance of cement grouted soil nails is still not well understood. This paper presents a typical field research program investigating axial strain and force distributions of cement grouted soil nails in several permanent highway cut slopes associated with slope depths, construction process, etc. The longitudinal strain and temperature changes of all these soil nails were measured with fiber Bragg grating (FBG) strain and temperature sensors, respectively. Typical measured results are summarized to investigate how axial forces of soil nails formed and developed after grouting. The possible ground movement inside slope and its effect on the axial strain results of soil nails are also interpreted and discussed.

FIELD CONDITIONS

Field monitoring projects were carried out on 7 permanent cut slopes along the highway from Panzhihua to Tianfang in Sichuan Province, China. These slopes were classified as four slope feature numbers, namely E1, E4, E5 and E6, which include 1, 2, 2, and 2 soil slopes, respectively. Slope heights of all these 7 slopes were 42.5 m (E1), 60 m and 46 m (E4), 55 m and 45 m (E5), and 52 m and 50 m (E6). The corresponding slope lengths were 230 m, 55 m, 45 m, 117 m, 73 m, 340 m and 215 m, respectively. Inclination angles of all these slopes were about 53° to horizontal after excavation work over the slope surface. The first group of monitoring data was collected on 21st May 2008 and the following strain and temperature data were collected almost monthly. Two sections in both slopes E1 and E4 and four slope sections in E5 and E6 were monitored. Diameters of all these steel bars were 32 mm except two steel bars in a slope section of E4. Field investigation works indicate that these slopes were mostly composed of typical completely decomposed granite (CDG) and highly decomposed granite (HDG). The 7 cut slopes were mainly stabilized using soil nails and anchors. Vertical and horizontal spacing between adjacent drill holes were 2 m. Inclination angle of the drill hole was 20° to horizontal. Soil nail lengths used for the reinforcement of these slopes were 15 m, 12 m, 9 m and 6 m, respectively. Figure 1 shows a schematic view of soil nail layout at a typical cross section of a slope. It is seen the slope is divided into two zone by the potential sliding surface, active zone and passive zone. The deep seated potential sliding surface was stabilized using relative long soil nails (generally 15 m), while short soil nails were used to stabilize the location where the potential sliding surface is shallow. FBG temperature and strain sensors were mostly adhered on the steel bar surfaces below the potential sliding surface monitoring axial strain distributions and corresponding temperature changes in the passive zone of the slope. Figures 1 also show a typical steel bar adhered with FBG sensors in cross sectional directions. It is seen the FBG sensor location oriented at the horizontal direction of the bar surface in order to minimize the possibility of measuring the bending strain, as the measurement method used by Thompson and Miller 1990; Turner and Jensen, 2005. Spacing between adjacent FBG sensors varies at 1.5 m or 2 m. A bottom sensing cable is connected to the sensor close to the nail tip. In case the sensing cable of the nail head is damaged, the reserved bottom sensing cable can still transmit signals of FBG sensors to data logger.

INSTALLATION OF FBG SENSORS

Installation work of FBG strain and temperature sensors is a crucial issue for the measurement of accurate strain and temperature data in this project. Essential measures were adopted in field to ensure all FBG strain sensors follow the deformation of steel bars well. A complete protection of sensors requires careful installation work as the FBG sensors are normally fragile particularly under complicated field conditions. Figures 2a to e show all installation procedures of FBG sensors in this field test. The main installation works of FBG sensors consist of:

(a) Preparation work of the steel bar surface (Figure 2a), such as the polish work of steel bar where the FBG sensors are mounted;
(b) Cleaning work of the steel bar surface with alcohol for the locations where the FBG strain and temperature sensors are mounted;
(c) Fixation of the two ends of a FBG strain sensor on the steel bar surface (Figure 2b) using instant glue;
(d) Fixation of the FBG strain sensor of the steel bar surface with epoxy resin;
(e) Adherence of FBG temperature sensor on nail bar surface using glue (Figure 2c);
(f) Adherence of the sensing cable on steel bar surface (Figure 2d); and
(g) Connection work of bottom sensing cable to the nail bar tip (Figures 2e).

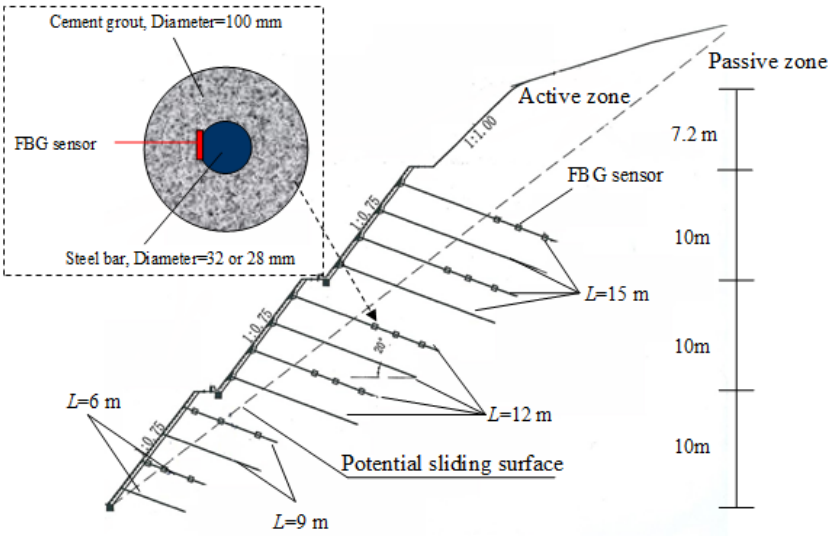

Figure 1. Schematic views of the location of FBG strain sensor in cross sectional area of the steel rebar and soil nail layout at a typical slope section

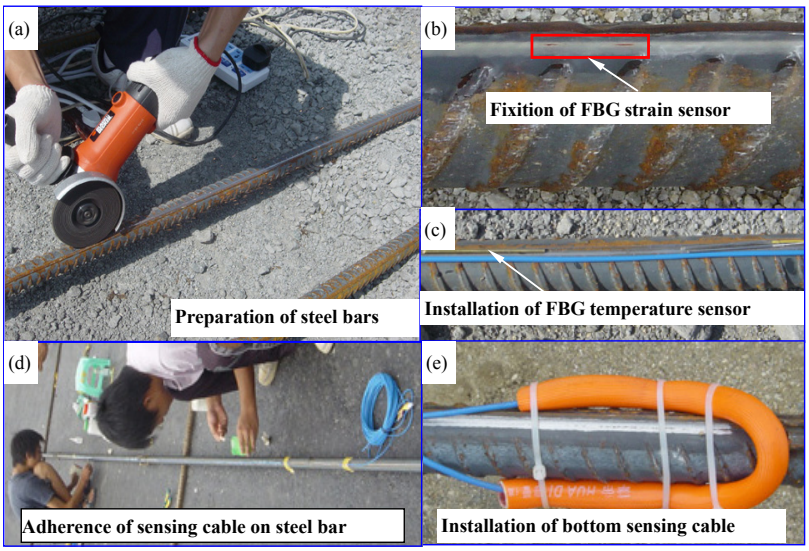

Figure 2. Installation of FBG sensors on the steel bar surface – (a) preparation of steel rebar; (b) fixation of strain sensor with epoxy resin; (c) installation of FBG temperature sensor; (d) adherence of sensing cable on the surface of steel rebar; and (e) installation of sensing cable at the bottom of the steel rebar.

It is noted that for the above procedures (b), (c) and (d), the steel bar surface must be cleaned before the fixation work of FBG strain and temperature sensors on the bar surface. In addition, the whole sensor section must be completely covered with epoxy resin (Figure 2b). The epoxy resin and the strain sensor could form an integrated body with the steel bar, and can follow the steel bar deformation well after around 24 hours. To make sure FBG sensors and the corresponding sensing cables would not be damaged under the complicated field environment or the possible significant disturbance during the installation process, essential protective measures have to be adopted in field. The FBG sensing cable was protected with a thin and narrow plastic layer on the steel bar surface. As this plastic layer is very thin, its effect on the mechanical performance of the steel bar/soil nail can be ignored. After the installation work of all FBG sensors, the steel bar was placed into a drill hole for grouting. Field experiences proved that the above field protection measures could effectively protect FBG sensors and sensing cables, especially when significant disturbance occurred during the installation process of steel bars or construction process of slope surface structures.

MONITORING RESULTS

Calculation of Axial Forces of Soil Nails

Axial tension force of all these soil nails can be obtained based on the measured pure strain data. Knowing the tensile strain ε of the steel bar, axial force can be calculated as below:

$$P = E_s A_s \varepsilon \tag{1}$$

where E_s and A_s denote the elastic modulus and cross section area of the steel bar, respectively. All axial force distribution of steel bars can be obtained using the above relationship. The yield force can be calculated by multiplying the yield stress with the cross sectional area of the steel bar. In case yield stress of steel bar is 200GPa. The yield force P_y of a steel bar is calculated as below:

$$P_y = A_s \sigma_y = \frac{\pi}{4} \times 32^2 \times 200 = 161\,\text{kN} \tag{2}$$

where A_s and σ_y denote the cross sectional area and yield stress of steel bar, and the corresponding units are mm^2 and kPa, respectively.

In this research project, all strain and temperature information was collected using optical fiber sensors. The strain and temperature changes lead to corresponding linear variations of central wavelength of FBG sensors, and this typical relationship is given as below:

$$\frac{\Delta\lambda_s}{\lambda_s} = C_\varepsilon \Delta\varepsilon + C_T \Delta T \tag{3}$$

where λ_s and $\Delta\lambda_s$ are the central wavelength of a FBG strain sensor and its change resulted from external temperature and strain changes. C_ε and C_T are both constant coefficients related to strain and temperature change, respectively. While the temperature sensor only reflects the external temperature change as follows:

$$\frac{\Delta\lambda_T}{\lambda_T} = C_T \Delta T \tag{4}$$

where λ_T and $\Delta\lambda_T$ are the central wavelength and its change of a FBG temperature sensor. Combing Eqs.3 and 4 yields the below relationship indicating the pure strain change with respect to the wavelengths of the FBG temperature and strain sensors:

$$\Delta\varepsilon = \frac{\Delta\lambda_s}{C_\varepsilon \lambda_s} - \frac{\Delta\lambda_T}{C_\varepsilon \lambda_T} \tag{5}$$

Since wavelengths or the wavelength changes of FBG temperature/strain sensors are recorded by the interrogator, the pure strain results of a soil nail can be directly obtained. The method of temperature compensation is suitable for all soil nails monitored in this field research project.

Analysis of Axial Force Results

All measured strain results can be used to calculate axial tension force of the soil nail bar by using Eq.1. Figures 3a and b show variations of axial force with time of soil nails E1-A2 and E1-A4. The strain measurement initiated immediately after grouting to observe the axial force development of inner steel bar with time. The distance (as marked in Figures 3a and b) indicates the distance between the strain sensor and the soil nail head. It is seen, most axial forces increase quickly in the initial one month, indicating that the hardening process of cement grout resulted in substantial rise of axial forces of steel bars. For example, the maximum axial forces increase from 0 to 4, 7 kN for nail bas in E1-A2, and E1-A4, respectively. This axial force increment may be the result of ground movement, or disturbance of construction works, etc. During this period, the bonding stress started to form between inner steel bar and surrounding soil. One month after grouting, axial forces still increase as time elapses until the mid-August then become stable. All the strain results or the calculated axial forces reflect the external ground movement and the effect of constructing nail heads or grid beams on the steel bar axial forces after cement grout has already hardened. For example, the slight changes of axial forces in the last two months in the above two figures indicate the slope movement is unobvious and therefore has limited effect on the axial forces of inner steel bars. In other words, the creep movement is weaker and weaker and finally become stable.

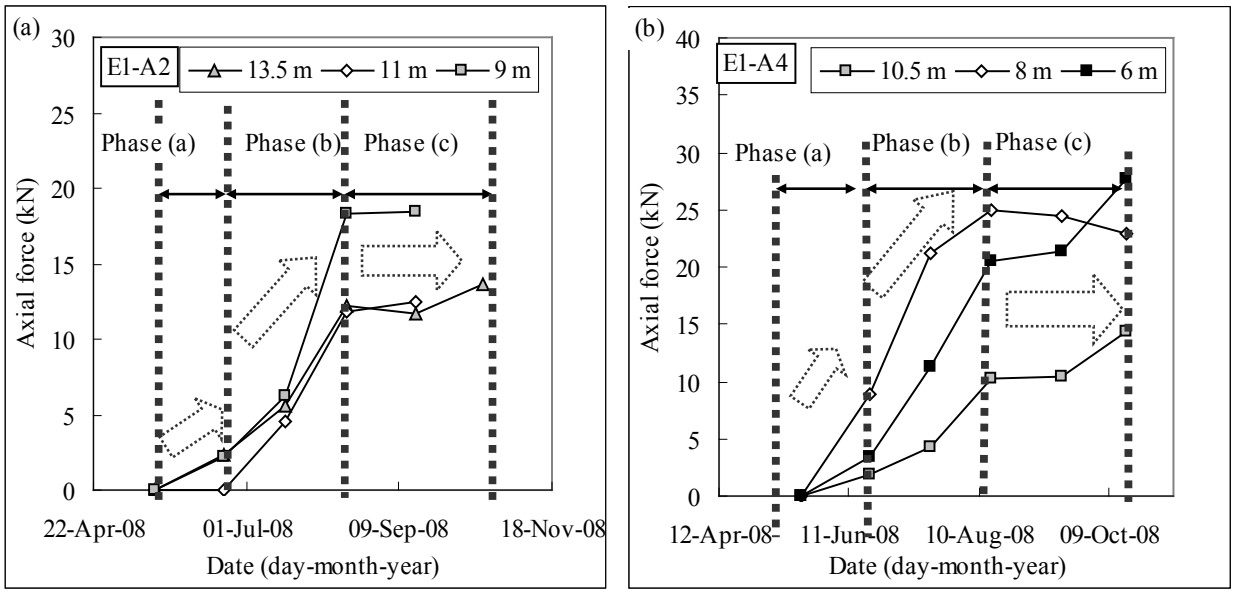

Figure 3. Variations of axial force against time at different sensor locations (a) E1-A2 (b) E1-A3 and (c) E1-A4

According to the above analysis, the post-grouting process of steel bars may be divided into three typical phases in this study, (a) the increase of axial tensile forces of steel bars under the hardening effect of cement grout, (b) the increase of axial forces of steel bars after the cement grout has already hardened, and (c) the phase with stable axial forces. The Phase (a) differs significantly from Phases (b) and (c) in the causes of stress re-distributions of steel bars. During the cement hardening process, i.e. Phase (a), bonding strength among steel bar, cement grout and external soil mass starts to build up which is therefore the dominant factor affecting the stress development of steel bars. One month after grouting, i.e. Phases (b) and (c), the cement grout has been fully hardened, allowing for external soil strain/stress transferred to the inner steel bar. Therefore, the occurred stress/strain of the inner steel bar is dependent on the practical ground movement.

Similar to the previous sections, all calculated axial force results of different sensor locations against time relationships from May 2008 to October 2008 are presented in Figures 4 a to d. It is clear that most axial forces in this slope section increase quickly in the initial one month after grouting, and most of these axial increments are below 15 kN. The hardening effect of cement grout starts to establish bonding effect between inner steel bars and surrounding soil through hardening effect, so that the corresponding soil movement would generate certain tension effect on the whole soil nail and therefore the increase of tension force of the inner steel bar. This is consistent with the observations in Figures 3 a and b, that is, the soil nail is still within phase (a). As the cement grout becomes harder and harder, the effect of soil movement becomes the dominant factor affecting the axial forces, but the axial forces become very stable for all the four soil nails in slope section E5-A, therefore, the related ground movement one month after grouting work may be unobvious.

Analysis and Discussions of the Maximum Strain Results of Soil Nails

To evaluate the soil nail behaviour at different slope heights in this study, the maximum soil nail strain at different slope locations are summarized and compared at different data collection date. Figures 5a to d show axial force variations of soil nails against slope height in two sections E5 and E6. These data were collected almost monthly. It is seen most axial forces of soil nails show substantial rise in the initial one month after grouting (marked as “one month after grouting” in Figures 5a to d), but mostly develop in a relative low rate as time further increases (E5-B, E6-A, and E6-C). For example, the maximum soil nail strain values are about 90 με for slope section E5-A and 110 με for slope section E5-B, both of which occur in the middle locations of this slope (within the height range of 25m to 35m). In addition, all measured strain change in the top and bottom parts of this slope appear not obvious and the maximum strain value is less than 40 με. As time elapses, the cement grout would become harder and harder, the external soil movement and inner steel bar would interact more and more closely due to the occurred bonding effect. The measured strain change appears to be smaller and smaller, indicating that the tension effect of these soil nails would be less obvious, as well as the whole slope may become relative stable as time elapses.

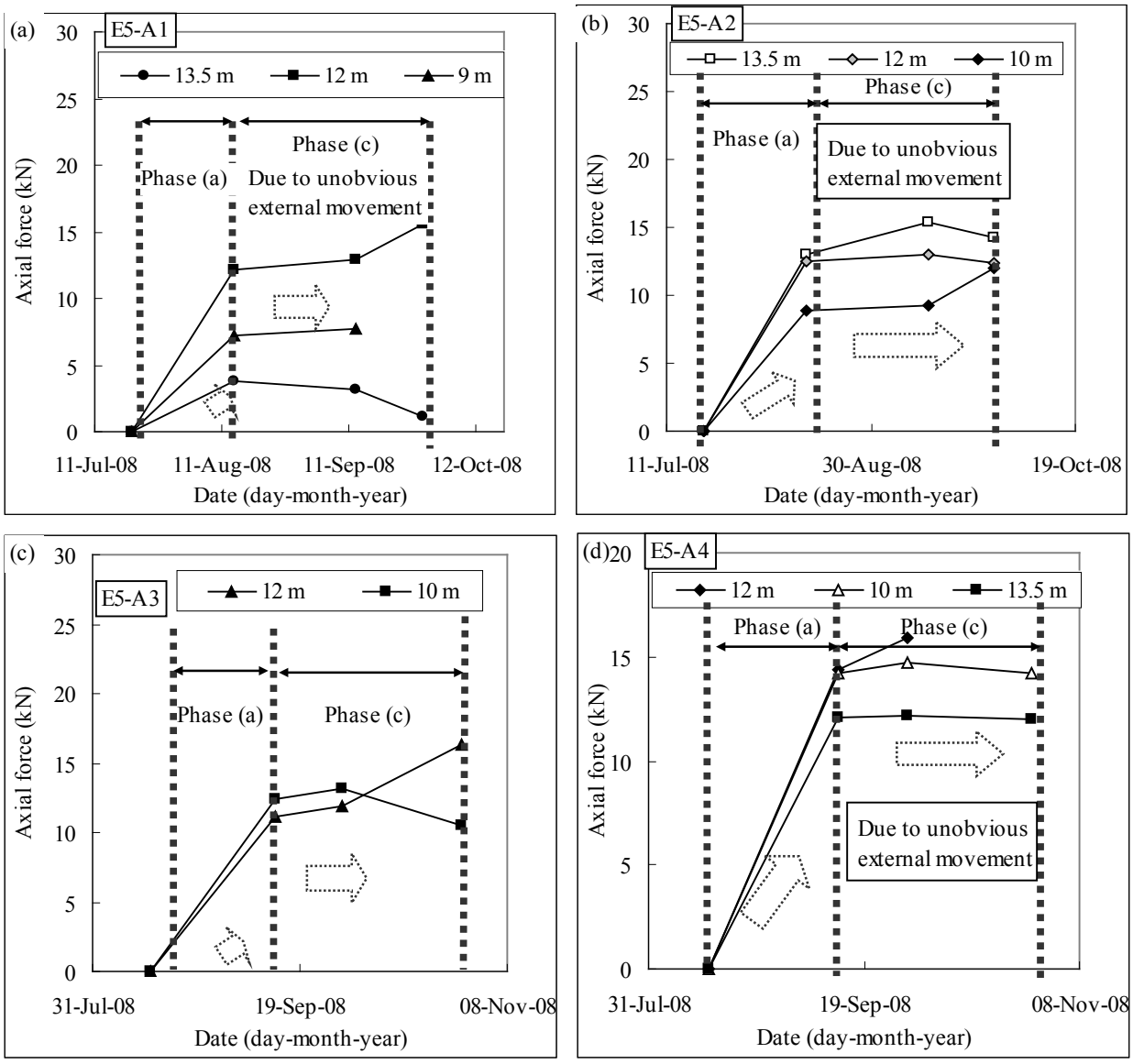

Figure 4. Axial force variations against time of soil nails in slope section E5 - (a) E5-A1; (b) E5-A2; (c) E5-A3; and (c) E5-A4

Relationships between the maximum strain values of soil nails against slope height of slope E6 are summarized in Figures 5 c and d. It is clear that the maximum strain increments of soil nails in the top location of slope section E6-A and in the middle location of slope section E6-C are more apparent than other slope locations. The measured maximum strain change in slope section E6-A is about 430 με, which presented at a slope height of 30 m. While the correspond data measured in slope section E6-C is about 100 με, occurred at the slope height of 30 m. These strain values increase to 500, 700, and 380, 400, 580 με, respectively, in the following two to three months. The observed regular strain variation trends of soil nails indicate that the slope movement (due to the external disturbance or the construction works) in the top location for slope section E6-A and the middle locations for slope section E6-A is more obvious than other slope locations. The initial quick strain increase demonstrates obvious ground movement, or construction work generates certain tension effect on the soil nails, such as the weight of grid beams on slope surface.

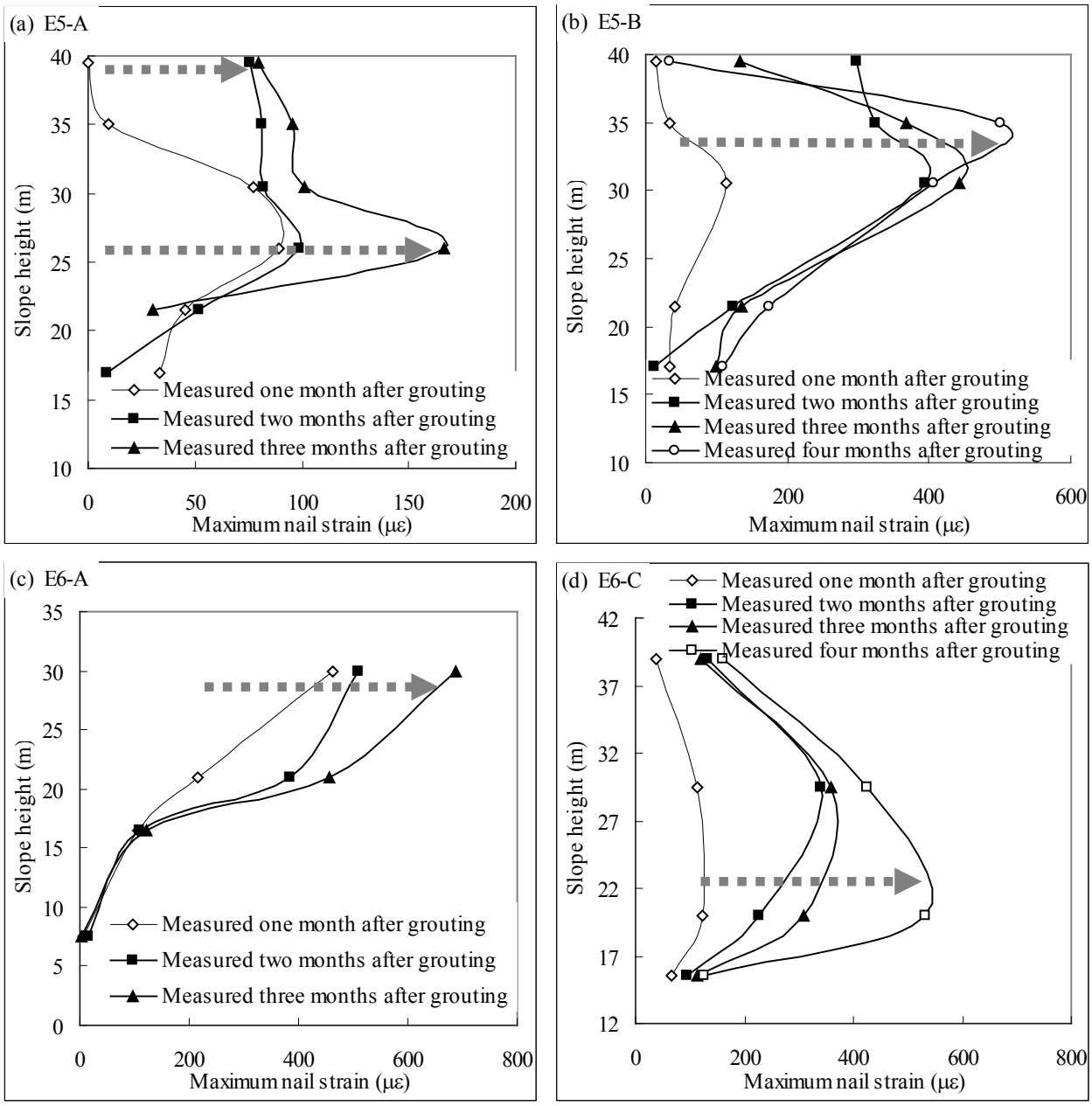

Figure 5. The maximum strain variations of soil nails against slope height at different measurement time for slope section – (a) E5-A; (b) E5-B; (c) E6-A; and (d) E6-C

The analysis of systematic strain changes of soil nails against soil nail depths is very critical particularly for the prediction of possible translational slide. In case the potential slide surface is straight and parallel to the slope surface, soil nails below the potential sliding surface would encounter a consistent tension effect, and this tension effect may occur at the same soil depth and finally generate a corresponding maximum axial tension forces at around the same soil depth. In this study, axial force variations against soil nail depths at two slope sections are summarized in Figure 6. The soil nail depth in this figure denotes the depth of a optical fiber strain sensor. It is seen most axial force results of steel bars are below a certain level (80 kN), which is also substantially lower than the yield force of the steel bar (161 kN). At the vertical depths lower than 10m, the axial forces are all almost lower than 50 kN, but still increase as time elapses. The initial axial forces are lowest among all axial force results. The tension effect in the middle part (around 8.2 m) of the first 10 m to the soil nail head is the most significant. However, for the remained 8 m part of this soil nail, the axial force increases sharply at around 14 m to the nail head, indicating that the tension effect is significant and this tension effect relaxes gradually as the sensor locations become deeper and deeper. These parts where the soil nail depths are within 10-14 m are subjected to slightly tension effect. To summarize, two obvious tension zones may be observed from the above data analysis, that is, the zones around 8.2 m and 14 m underground, this indicates that the mechanical behavior of soil nails underground is complex at different locations.

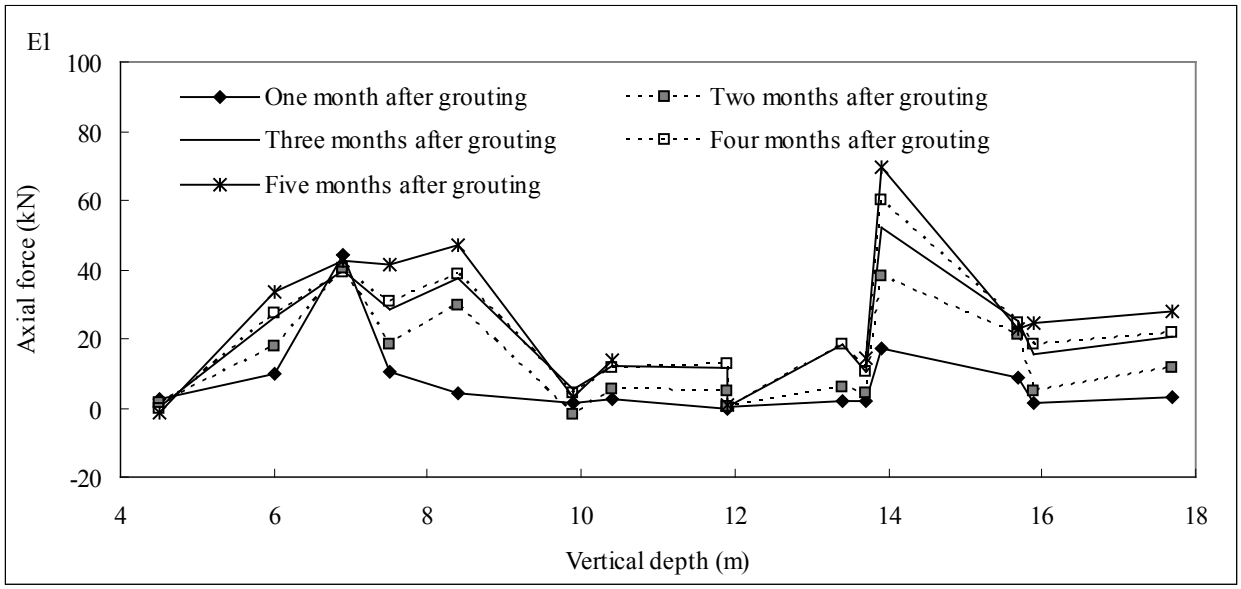

Figure 6. Relationships between axial force variations and vertical depth of soil nail in slope section E1.

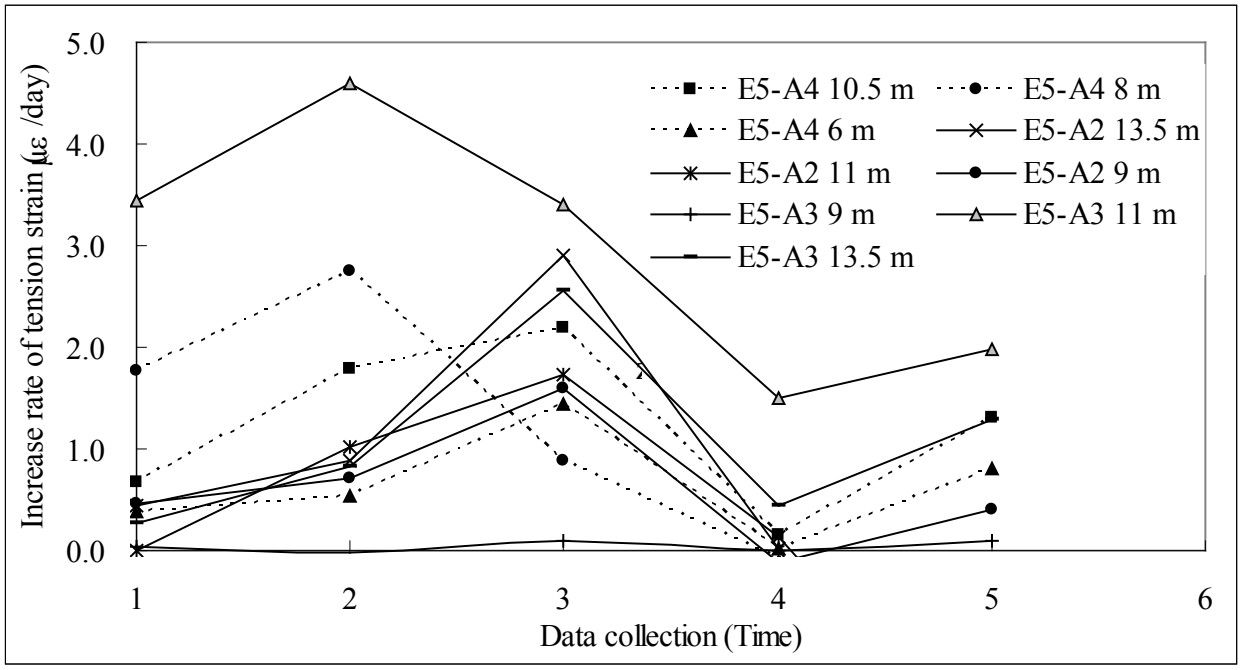

Figure 7. Variations of increasing rates of soil nails against time in different sections of slope E5

To further investigate the strain variations in details after grouting work, typical increase rates of tension strain of different soil nails in slope section E5-A are summarized in Figure 7. This increase rate is calculated by dividing total strain increment with time interval. "E5-A1" as marked in this figure indicates the soil nail number, while the distance value in the figure shows the distance between the sensor location and the soil nail head. It is clear most increase rates of tension strain appear to low, at a rate of normally less than 4 με daily. All increase rates of tension strain appear to increase in the first three data collection times after grouting work except two soil nails, E5-A3 11m, and E5-A4 8m. These increase rates become lower and lower as time further elapses, and finally stabilize at a level less than 2 με each day. The initial relative high increase rate of tension strain may be due to the highly disturbance from construction works slope or the creep movement of slopes. As time passes by, the tension strain increments become lower and lower, and finally maintain at a relative stable level. That is, the creep movement of the whole slope or other factors generating tension effect of soil nails becomes weaker and weaker as time elapses.

Inner Temperature Changes of Soil Nails

Temperature variations of steel bars have effects on the strain change (thermal effect) after grouting, so that the related temperature measurement using sensors is essential. In this project, typical relationships of temperature variations against time of soil nails in slope sections E6 are summarized in Figure 8. "Top and bottom" in this figure indicate the temperature sensor location is close to the soil nail head and tip, respectively. It is clear most temperature changes increase slightly from June to September in slope section E6-A, where the maximum temperature change is quite limited (less than 2 degree for section E6-A). The temperature sensor on soil nail E5-A4 shows the maximum temperature increase but is still less than 2 degree. While for the slope section E6-B, the maximum temperature change appear to be more obvious than that of slope section E6-A, with a maximum temperature change around 4 degree being obtained on soil nail E6-B5. These measured temperature data drop substantially in October where the maximum temperature reduction is around 4 degree. This is possible due to that the winter comes closer and closer, so that the temperature becomes lower and lower. This temperature reduction would have substantial thermal effect on the measured strain data, so that the temperature compensation is very essential in this project. The limited temperature change may be because the temperature sensors are deep seated and therefore insensitive to the external temperature changes of field environment.

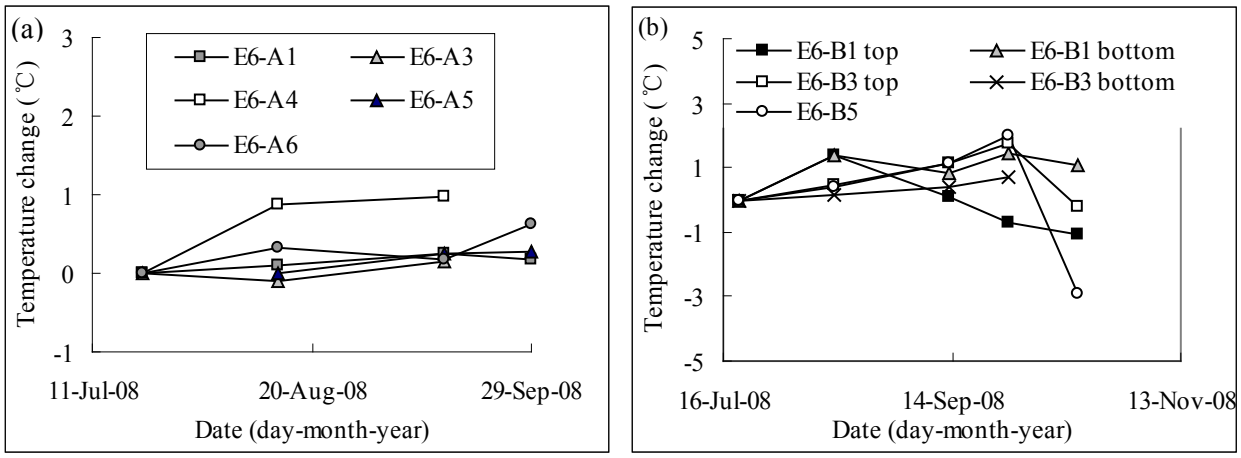

Figure 8. Measured temperature changes against time in slope sections - (a) E6-A; and (b) E6-B

SUMMARY AND CONCLUSIONS

A field monitoring research program is presented to study the behaviour of about 50 cement grouted soil nails in a number of high way cut slopes. In this study, fiber Bragg grating (FBG) sensors were adopted and used to measure strain and temperature changes of soil nails. All strain and temperature variations associated with time and the calculated axial forces are presented to analyze the mechanical behaviour of soil nails. All these data and related observations are summarized, compared and discussed in this paper and typical conclusions are summarized as follows:

1. After cement grout has hardened, the transferred axial force from surrounding soil to the inner nail bar is time dependent. The continuous increase of the axial tensile force indicates that the soil nail is subjected to progressive "pullout" effect, which is virtually triggered by the ground movement of the slope. This also demonstrates that the soil nail behaviour is passive rather than positive.
2. The post-grouting process of steel bars may be divided into three typical phases, (a) the increase of axial tensile forces of steel bars under the hardening effect of cement grout, (b) the increase of axial forces of steel bars after the cement grout has already hardened, and (c) the phase with stable axial forces.
3. The measured maximum axial strain results of steel bars vary systematically and regularly with respect to slope height. Significant rise of axial tensile strain indicates apparent ground movement inside the slope. The increase of axial strain/force at slope toes is generally less distinct compared to the strain results in the middle and top locations of slopes according to the monitored results.
4. Increase rate of tension strain appears to behave systematically and consistently in this study. The initial increase rate of tension strain is relative high, but as time elapses, the related increase rate of tension strain becomes lower and lower and finally maintain at a relative low level.
5. Temperature changes of soil nails are within a limited range, this may be due to that most FBG temperature sensors are deep seated underground so that insensitive to the temperature change of external environment.

ACKNOWLEDGMENTS

The authors gratefully acknowledge the financial supports provided by the STU Scientific Research Foundation for Talents (SRFT) (Project No: NTF12015) and by the joint funding (A/C:5-ZJE2) of Construction Industry Institute (Hong Kong) Limited and the Faculty of Construction and Environment of The Hong Kong Polytechnic University.

REFERENCES

Cheung, R.W.M.. and Lo, D.O.K. (2011). "Use of time-domain reflectometry for quality control of soil-nailing works", *Journal of Geotechnical and Geoenvironmental Engineering*, 137(12), 1222-1235.

Chu, L.M. and Yin, J.H. (2005). "Comparison of interface shear strength of soil nails measured by both direct shear box tests and pullout tests", *Journal of Geotechnical and Geoenvironmental Engineering*, 131(9), 1097-1107.

Chu, L.M. and Yin, J.H. (2005). "A laboratory device to test the pull-out behavior of soil nails", *ASTM geotechnical testing journal*, 28(5), 499-513.

Hong, C.Y., Yin, J.H., Jin, W., Wang, C., Zhou, W.H. and Zhu, H.H. (2010). "Comparative study on the elongation measurement of a soil nail using optical lower coherence interferometry method and fbg method", *Advances in Structural Engineering*, 13(2), 309-319.

Jewell, R.A. (1991). "Review of theoretical-models for soil nailing", *Performance of Reinforced Soil Structures*, 265-275.

Jewell, R.A. (1991). "Soil nailing", *Performance of Reinforced Soil Structures*, 197-200.

Klar, A., Bennett, P.J., Soga, K., Mair, R.J., Tester, P., Fernie, R., St John, H.D. and Torp-Peterson, G. (2006). "Distributed strain measurement for pile foundations", *Proceedings of the Institution of Civil Engineers-Geotechnical Engineering*, 159(3), 135-144.

Mohamad, H., Soga, K., Pellew, A. and Bennett, P.J. (2011). "Performance monitoring of a secant-piled wall using distributed fiber optic strain sensing", *Journal of Geotechnical and Geoenvironmental Engineering*, 137(12), 1236-1243.

Plumelle, C., Schlosser, F., Delage, P. and Knochenmus, G. (1990). "French national research-project on soil nailing - clouterre", *Design and Performance of Earth Retaining Structures*, 25, 660-675.

Su, L.J., Chan, T.C.F., Shiu, Y.K., Cheung, T. and Yin, J.H. (2007). "Influence of degree of saturation on soil nail pull-out resistance in compacted completely decomposed granite fill", *Canadian Geotechnical Journal*, 44(11), 1314-1328.

Su, L.J., Chan, T.C.F., Yin, J.H., Shiu, Y. and Chiu, S. (2008). "Influence of overburden pressure on soil–nail pullout resistance in a compacted fill", *Journal of Geotechnical and Geoenvironmental Engineering*, 134, 1339.

Sun, A., Semenova, Y., Farrell, G., Chen, B., Li, G. and Lin, Z. (2010). "Botdr integrated with fbg sensor array for distributed strain measurement", *Electronics Letters*, 46(1), 66-67.

Thompson, S.R. and Miller, I.R. (1990). "Design, Construction and Performance of a Soil Nailed Wall in Seattle, Washington", *Design and Performance of Earth Structures, ASCE Geotechnical Publication*, No. 25, 629-643.

Turner, J.P. and Jensen, W.G. (2005). "Landslide stabilization using soil nail and mechanically stabilized earth walls: Case study", *Journal of Geotechnical and Geoenvironmental Engineering*, 131(2), 141-150.

Wu, Z.S., Xu, B., Takahashi, T. and Harada, T. (2008). "Performance of a botdr optical fibre sensing technique for crack detection in concrete structures", *Structure and Infrastructure Engineering*, 4(4), 311-323.

Yin, J.H. and Zhou, W.H. (2009). "Influence of grouting pressure and overburden stress on the interface resistance of a soil nail", *Journal of Geotechnical and Geoenvironmental Engineering*, 135(9), 1198-1208.

Yin, X.H. and Su, L.J. (2006). "An innovative laboratory box for testing nail pull-out resistance in soil", *Geotechnical Testing Journal*, 29(6), 451-461.

Zhang, L.L., Zhang, L.M. and Tang, W.H. (2009). "Uncertainties of field pullout resistance of soil nails", *Journal of Geotechnical and Geoenvironmental Engineering*, 135(7), 966-972.